Advances in the Science and Engineering of Casting Solidification
Edited by: Laurentiu Nastac, Baicheng Liu, Hasse Fredriksson, Jacques Lacaze, Chun-Pyo Hong, Adrian V. Catalina, Andreas Buhrig-Polaczek, Charles Monroe, Adrian S. Sabau, Roxana Elena Ligia Ruxanda, Alan Luo, Subhayu Sen, and Attila Diószegi
TMS (The Minerals, Metals & Materials Society), 2015

DEPENDENCE OF HARDNESS ON MICROSTRUCTURE OF A DIRECTIONALLY SOLIDIFIED Sn-40wt.%Bi-0.7wt.%Cu ALLOY

Bismarck Luiz Silva [1] and José Eduardo Spinelli [1]

[1] *Department of Materials Engineering, Federal University of São Carlos – UFSCar, Washington Luis Rd, km 235, 13565-905, São Carlos, São Paulo, Brazil*

Keywords: Sn-Bi-Cu alloys; microstructure; hardness.

Abstract

Continuous efforts in replacing Sn-Pb eutectic solder have been attempted. Sn-Bi alloys are candidates as lead-free solders for low temperature soldering due to its adequate cost and general consistency. Additions of Cu within these alloys can improve the ductility, mechanical strength and wettability. Nevertheless, a deeper study considering the characterization of the as-soldered ternary Sn-40wt%Bi-0.7wt%Cu microstructures remains still to be performed. Thus, the present experiments were carried out by directional solidification (DS) of the Sn-40Bi-0.7Cu with a view to establish experimental interrelations involving solidification thermal parameters (growth rate - V_L and cooling rate - $\dot{T}_L$) with some microstructure features (λ_2). The experimental relations obtained for this alloy have been compared with those already determined for the binary Sn-0.7wt.%Cu and Sn-40wt.%Bi alloys. The microstructures from the bottom to the top along the Sn-Bi-Cu alloy were entirely dendritic. Further, a Hall-Petch equation is proposed relating HV to λ_2 for the Sn-40Bi-0.7Cu alloy.

INTRODUCTION

Due to the inherent toxicity of lead (Pb), environmental regulations around the world have been targeted to eliminate the usage of Pb-bearing solders in electronic assemblies. This has prompted the development of ‘‘Pb-free’’ solders, that’s why that the research activities in this field have been developed [1-3].

There are strict performance requirements for solder alloys used in microelectronics. In general, the solder alloy must meet the expected levels of reliability and mechanical properties (as the hardness), as well as electrical and mechanical performance. Within this framework, Sn-Bi [2,4,5,6] and Sn-Cu eutectic [7-9] arise as promising Pb-free alternative due characteristics as low melting point, low cost, low dissolution of Cu substrate and feasible for soldering processes.

According to Zu and co-authors [6] the *liquidus* temperature (T_L) and eutectic temperature (T_E) for hypoeutectic Sn-40wt%Bi alloy are 169.5°C and 136.5°C, respectively, whereas Osório *et al.* [4] cite T_L=172°C and T_E=136°C. This latter work showed that the microstructure of the Sn-40wt%Bi is constituted of Sn-rich dendritic matrix and a eutectic mixture in the interdendritic regions. However, some studies [6,10] showed that microstructure for this binary is composed by Sn-rich matrix with Bi precipitates embedded inside this structure and eutectic mixture with alternate-layered lamellar structure.

Meanwhile, the Sn-Cu eutectic reaction is between a faceted intermetallic Cu_6Sn_5 phase and a non-faceted Sn-rich phase and occurs at 227°C. During the eutectic reaction, the Cu_6Sn_5 phase grows as rod-like embedded in a continuous Sn-rich matrix [9,11]. Further, recent studies [12,13] of the directional solidification under unsteady-state conditions showed that eutectic Sn-Cu alloy can exhibit both dendritic structure and cell (eutectic colonies) structures, depending of the cooling rates, with primary Cu_6Sn_5 intermetallic particles dispersed in a Sn-rich matrix. Others works [7,8] also have described similar structures for Sn-0.7wt%Cu solder.

Despite presenting some advantages such as low melting point, the hypoeutectic Sn-40wt%Bi yet need to improve others important properties for application in the electronics industry as UTS-Ultimate Tensile Strength, YS-Yield Tensile Strength, Ductility, Hardness, Wettability, Electrical and Thermal conductivity, Corrosion and Fatigue Resistance. Under this context, few references of literature [14-17] indicate that additions of Cu on binary Sn-Bi solders may promote significant enhancements in the properties listed above, emerging as an alloy of high potential for soldering operations. Typical microstructures for ternary Sn-40wt%Bi-0.1wt%Cu solder were reported for Takao et al [17]. The microstructures are quite similar those obtained for Sn-40wt%Bi solders, but with a presence of primary Cu_6Sn_5 intermetallic particles both in the Sn-Bi eutectics and Sn-rich phase.

Therefore, this study focuses on the influences of the thermal parameters, growth rate – V_L and cooling rate – $\dot{T}_L$, in the evolution of secondary dendritic spacing (λ_2) in the Sn-40wt%Bi-0.7wt%Cu solder solidified under unsteady-state conditions, which in turn was correlated with Vickers hardness (HV) values along of the Sn-Bi-Cu alloy ingot. A Hall-Petch relation between HV and λ_2 was discussed.

EXPERIMENTAL PROCEDURE

The Sn-40wt%Bi-0.7wt%Cu solder alloy was prepared using 99.94% pure tin, 99.98% pure bismuth and 99.94% pure copper. Heat is directionally extracted only through a water-

cooled bottom made of low carbon steel (SAE 1020), promoting vertical upward directional solidification. The casting assembly used in the solidification experiment is reported in previous works [18-20]. Continuous temperature measurements in the casting were performed during solidification by fine type J thermocouples (0.2 mm diameter wire sheathed in 1.0mm outside diameter stainless steel tubes) placed along the casting length.

The cylindrical ingot was sectioned along its vertical axis so that longitudinal and transverse samples could be obtained. Selected transverse (perpendicular to the growth direction) and longitudinal sections of the directionally solidified Sn-Bi-Cu casting at different positions from the metal/mold interface were polished and etched (solution of 2mL HCl, 10mL $FeCl_3$ and 100mL H_2O) for metallography. An optical image processing system Olympus, GX51 (Olympus Co., Japan) and Field Emission Gun (FEG) - Scanning Electron Microscope (SEM) Philips (XL30 FEG) were used to acquire the images.

The secondary dendritic arm spacing (λ_2) was measured on longitudinal section of the casting through of intercept method [21]. At least 35 measurements were performed for each selected position. X-ray diffraction (XRD) measurements were carried out with a view to determining the phases forming the Sn-40wt%Bi-0.7wt%Cu as-cast microstructure. XRD patterns were obtained with a 2-theta range from 20° to 90°, Cu-Kα radiation with a wavelength, λ, of 0.15406 nm.

Before hardness tests the specimen surfaces were polished with fine sandpaper to remove any machining marks, polished and etched (same etchant solution cited earlier). Hardness Vickers tests were performed (according to the ASTM E 384-11 standard) on the longitudinal sections of the samples by using a test load of 500g and a dwell time of 15s. The evaluated positions were 5.0mm, 15.0mm, 20.0mm, 25.0mm, 40.0mm, 50.0mm and 70.0mm from cooled surface of the casting. A Shimadzu HMV-G 20ST model hardness measuring tester was used. The average of at least 5 measurements on each sample was adopted as the hardness value of a representative position.

RESULTS AND DISCUSSIONS

Figure 1 shows the macrostructure of the Sn-40wt%Bi-0.7wt%Cu solder casting and typical longitudinal microstructures obtained after metallographic examination. Columnar grains prevailed along the directionally solidified casting, which means that vertically aligned grains have grown from the bottom of the casting. The dendritic growth prevailed along entire casting. It can be seen a gradual increase of secondary dendritic arm (λ_2) due to decreased of cooling rates ($\dot{T}_L$) and growth rate (V_L) in the progress of directional solidification.

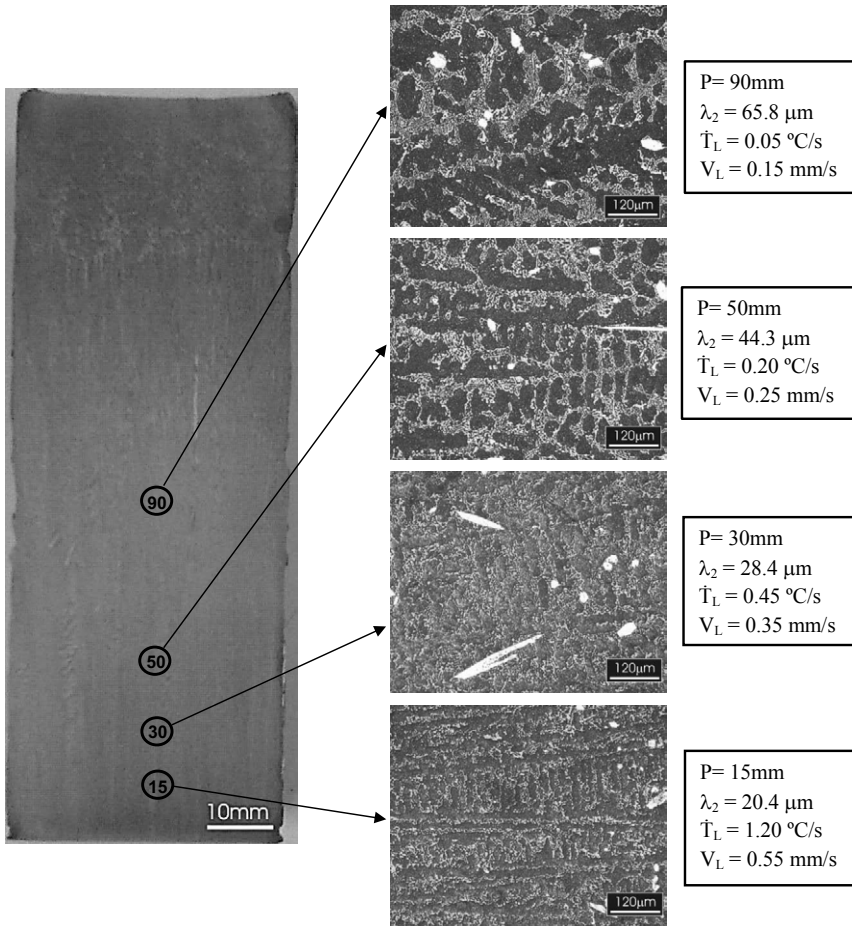

Figure 1. Macrostructure and longitudinal microstructures of the Sn-40wt%Bi-0.7wt%Cu alloy casting. "P" is the position from the metal/mold interface. The black arrows indicate the microstructures (longitudinal section) correspondents for each position observed.

Microstructures of the transverse section show the constituent phases of ternary Sn-Bi-Cu (Figure 2a). It was found that the as-cast microstructure was arranged by Sn-rich dendrites surrounded with a eutectic mixture (Bi-rich and Sn-rich phases). Further, the Sn-rich dendrites were found to be decorated with Bi precipitates in their own core. The primary Cu_6Sn_5 intermetallic particles (indicated by gray arrow) are non-homogeneously distributed along the microstructure. This result is also according with predicted by Takao et al [17]. Figure 2b shows the X-ray diffractograms for the ternary Sn-Bi-Cu solder and the presence of peaks associated with the Cu_6Sn_5 and Cu_3Sn intermetallics compounds (IMCs), Sn-rich and Bi-rich phases in the examined positions from the metal/mold interface. Although the Cu_3Sn particles could not be identified by microscopy, characteristic X-ray peaks were identified. Also, the

X-ray spectra show that the Sn-rich and the Bi-rich phases corresponding peaks' intensities are increased and decreased, respectively, as cooling rate is decreased.

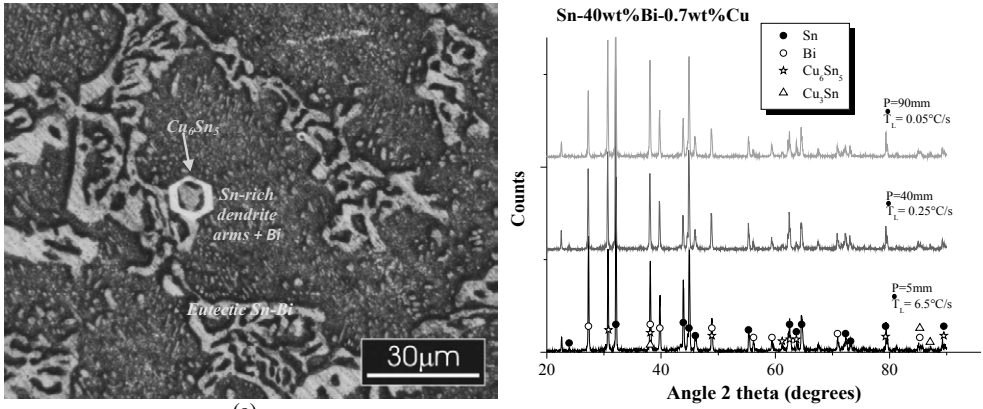

Figure 2. (a) Microstructure emphasizing the phases formed in the Sn-40wt%Bi-0.7wt%Cu solder alloy; (b) X-ray diffraction (XRD) patterns of Sn-40wt%Bi-0.7wt%Cu solder samples for different positions along the directionally solidified casting length.

From the thermal readings during directional solidification is possible to obtain a power function, position from the metal/mold interface *vs* time of the *liquidus* isotherm (T_L=165.6°C) front passing by each thermocouple. The derivative of this function with respect to time gave values for the tip growth rate (V_L), as shown in Figure 3a. The experimental cooling rate (Fig. 3b) was determined by considering the thermal data recorded immediately after the passing of the *liquidus* front by each thermocouple. As the solidification front advances, the values of both V_L and $\dot{T}_L$ decrease. This effect is reversely translated resulting in increasing of secondary dendritic arm spacing (see Figure 1). Additionally, it can be observed that the V_L and $\dot{T}_L$ experimental values for eutectic Sn-0.7Cu and for the ternary Sn-Bi-Cu directionally solidified solders are similar, whereas the binary Sn-Bi alloy presented a range of values much greater than those cited. This fact indicates that the addition of 0.7Cu in the eutectic Sn-40Bi tends to decrease remarkably the metal/mold thermal conductance efficiency, which could be intimately related with interfacial conditions and affinity between molten alloys and substrate. In the case of the two binary alloys inserted for comparison purposes the water-cooled bottom was also made of low carbon steel (SAE 1020). The experimental fittings were inserted to indicate possible values considering positions which were not monitored within the castings.

The secondary dendritic arm (λ_2) dependence on the growth rate (V_L) for the ternary Sn-Bi-Cu alloy is shown in Figure 4, which present the average spacing and their minimum and maximum values. The line represents empirical power law which fit the experimental scatter. It can be seen that λ_2 variation with the tip growth rate (V_L) is characterized by -2/3 exponent, which show that the increased of V_L, λ_2 values decreases. This exponent seems to represent reasonably the Sn-40wt%Bi-0.7wt%Cu solder and it has been reported for similar correlations concerning Sn-Pb [22], Pb-Sb [20], Al-Fe [19] and Sn-Cu [12] alloys. Experimental model of Sn-40wt%Bi solder [4] also solidified under unsteady-state conditions

was inserted in the graph (Figure 4), having a -2/3 exponent. Figure 4 shows that for a same V_L value, lower λ_2 measurements have been achieved for ternary Sn-Bi-Cu, indicating that the addition of cooper (Cu) may be beneficial for microstructure refinement.

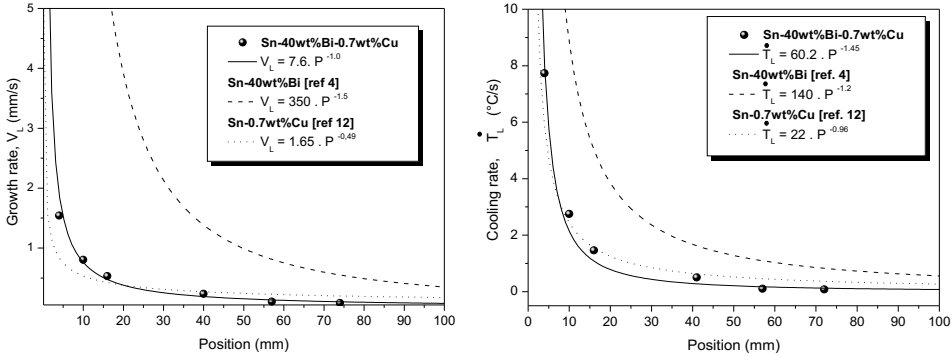

Figure 3. Experimental values of (a) growth rate and (b) cooling rate versus position along the casting length for the Sn-0.7wt%Cu, Sn-40wt%Bi and Sn-40wt%Bi-0.7wt%Cu solder alloys.

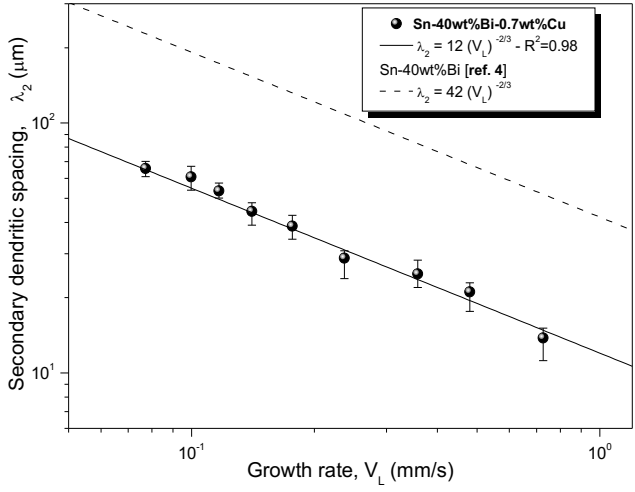

Figure 4. Secondary dendritic arm (λ_2) as a function of growth rate (V_L) for the directionally solidified Sn-40wt%Bi-0.7wt%Cu alloy casting. R^2 is the coefficient of determination.

It is known that the level of hardness is affected by phases and their size and distribution in the microstructure. Thus, Figure 5 shows a classical Hall-Petch relationship between hardness Vickers and the inverse square root of λ_2 obtained for the Sn-Bi-Cu alloy. The experimental expression $HV = 6.1 + 39.5\ \lambda_2^{-1/2}$ is able to represent the hardness behavior of the ternary Sn-40wt%Bi-0.7wt%Cu solder alloy with evolution of λ_2. It can be seen that the

HV measurements remarkably increase with decreasing secondary dendritic arm spacing. This is due to the better distribution of the reinforcing phases such as the eutectic Sn/Bi mixture associated with lower secondary dendrite arm spacing as can be seen in the microstructures inserted in Figure 5. Increase on hardness can also be attributed to smaller Bi precipitates within the dendritic matrix developed for positions near the cooled surface of the Sn-Bi-Cu alloy casting. Average hardness values about 19HV are associated with a mean λ_2=11μm while a value of 11.5HV refers to λ_2 of 61μm.

Hardness values found in this study are higher than those obtained for eutectic Sn-37%Pb solder [23], showing that Sn-40wt%Bi-0.7wt%Cu solder may be an alternative to replace the Sn-Pb alloys in applications that hardness is required.

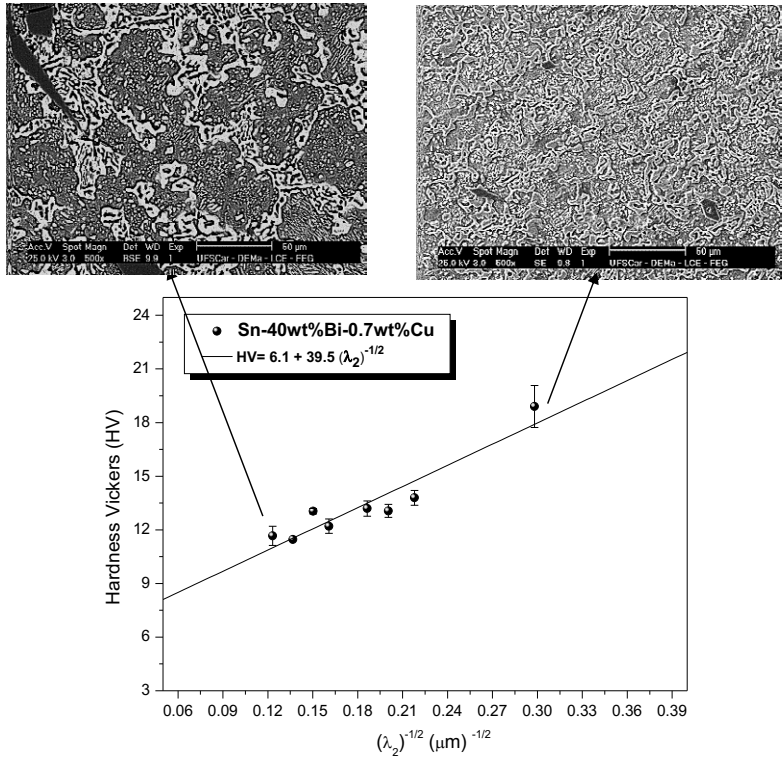

Figure 5. Hardness Vickers (HV) against (a) $\lambda_2^{-1/2}$ for Sn-40wt%Bi-0.7wt%Cu solder.

CONCLUSIONS

A microstructural dendritic matrix prevailed in the entire DS Sn-40wt%Bi-0.7wt%Cu alloy casting. The eutectic mixture located in the interdendritic regions is shown to be formed by Sn-rich and Bi-rich. Also, the dendrites were found to be decorated by Bi particles. Cu_6Sn_5 IMCs were seen non-homogeneously dispersed in both the eutectic Sn-Bi and the Sn-rich dendrites.

As the solidification front advances the experimental solidification cooling rate ($\dot{T}_L$) and growth rare (V_L) tend to shorten. The secondary dendritic arm spacing (λ_2) decreases as the growth rate V_L increases. Hardness changes remarkably along the Sn-Bi-Cu alloy casting, with higher values connected with the fineness of microstructure and of the eutectic mixture. Such refinement allows a homogeneous distribution of the eutectic and it is translated by the secondary dendritic spacing. It was found that a classical Hall-Petch correlation ($HV= 6.1 + 39.5\ \lambda_2^{-1/2}$) fit adequately the experimental scatter.

ACKNOWLEDGEMENTS

The authors acknowledge the financial support provided by FAPESP (São Paulo Research Foundation, Brazil: grants 2013/13030-5 and 2013/08259-3).

REFERENCES

[1] M. Abtew, G. Selvaduray, **"**Lead-free Solders in Microelectronics", *Materials Science and Engineering*, 27 (2000), 95-141.
[2] T Laurila, V Vuorinen, JK Kivilahti, "Interfacial reactions between lead-free solders and common base materials", *Materials Science and Engineering*, R 49 (2005), 1-60.
[3] N Pareck, "Parts and Packaging Program, United State America". *Nasa: Lead-free solders*, Goddard Space Flight Center, Greenbelt, Maryland, 1996.
[4] WR Osorio, LC Peixoto, LR Garcia, N Mangelinck-Noel, A Garcia, "Microstructure and mechanical properties of Sn-Bi, Sn-Ag and Sn-Zn lead-free solder alloys", *Journal of Alloys and Compounds*, 572 (2013), 97-106.
[5] Y Goh, ASMA Haseeb, MFM Sabri, "Effects of hydroquinone and gelatin on the electrodeposition of Sn-Bi low temperature Pb-free solder", *Electrochimica Acta*, 90 (2013) 265-273.
[6] F Zu, B Zhou, X Li, X Yi, Y Chen, Q Sun, **"**Effect of liquid-liquid structure transition on solidification of Sn-Bi alloys", *Transactions of Nonferrous Metals Society of China*, 17 (2007), 893-897.
[7] K. Nogita, J. Read, T. Nishimura, K. Sweatman, S. Suenaga and A. K. Dahle, **"**Microstructure control in Sn-0.7wt%Cu alloys", *Materials Transactions*, 46 (2005) 2419-2425.
[8] T Ventura, C Gourlay, K Nogita, T Nishimura, M Rappaz, AK Dahle, **"**The influence of 0-0.1wt% Ni on the microstructure and fluidity length of Sn-0.7Cu-xNi", *Journal of Electronic Materials*, 37 (2008), 32-39.
[9] K Nogita, "Stabilization of Cu6Sn5 by Ni in Sn-0.7Cu-0.05Ni lead-free solder alloys", *Intermetallics*, 18 (2010), 145-149.
[10] L Chen, P Septiwerdani, Z Chen, **"**Elastic modulus, hardness and creep performance of SnBi alloys using nanoindentation", *Materials Science & Engineering A*, 558 (2012), 253-258.

[11] AA El-Daly, AE Hammad, "Development of high strength Sn-0,7Cu solders with the addition of small amount of Ag and In", *Journal of Alloys and Compounds*, 509 (2011) 8554-8560.
[12] ITL Moura, CLM. Silva, N Cheung, P R Goulart, A Garcia, J E Spinelli, **"**Cellular to dendritic transition during transient solidification of a eutectic Sn-0.7wt%Cu solder alloy", *Materials Chemistry and Physics*, 132 (2012), 203-209.
[13] BL Silva, N Cheung, A Garcia, JE Spinelli, Thermal Parameters, Microstructure, and Mechanical Properties of Directionally Solidified Sn-0.7wt%Cu Solder Alloys Containing 0 ppm to 1000 ppm Ni, *Journal of Electronic Materials*, 42 (2013) 179-191.
[14] X Hu, K Li, Z Min, "Microstructure evolution and mechanical properties of Sn0.7Cu0.7Bi lead-free solders produced by directional solidification", *Journal of Alloys and Compounds*, 566 (2013) 239-245.
[15] J Xu, Q Hu, H He, F Zhang, Z Zhao, "Study of Sn-Bi-Cu Lead-free Solder". Proceedings of 10th Electronics Packaging Technology Conference, (2008) 1375-1380.
[16] L Zang, Z Yuan, H Zhao, X Zhang, "Wettability of molten Sn-Bi-Cu solder on Cu substrate", *Materials Letters*, 63 (2009) 2067-2069.
[17] H Takao, A Yamada, H Hasegawa, "Mechanical properties and solder joint reliability of low-melting Sn-Bi-Cu lead free solder alloy". R&D Review of Toyota CRDK, 39 (2004).
[18] MV Cante, JE Spinelli, IL Ferreira, N Cheung, A Garcia, "Microstructural development in Al-Ni alloys directionally solidified under unsteady-state conditions". *Metallurgical and Materials Transactions A*, 9 (2008), 1712-1726.
[19] PR Goulart, KS Cruz, JE Spinelli, IL Ferreira, N Cheung, A Garcia, "Cellular growth during transient directional solidification of hypoeutectic Al-Fe alloys", *Journal of alloys and compounds*, 470 (2009), 589-599.
[20] DM Rosa, JE Spinelli, IL Ferreira, N Cheung, A Garcia, "Cellular/dendritic transition and microstructure evolution during transient directional solidification of Pb-Sb alloys", *Metallurgical and Materials Transactions A*, 39A (2008), 2161-2174.
[21] DG McCartney, JD Hunt, "Measurements of cells and primary dendrite arm spacing in directionally solidified aluminium alloys", *Acta Metallurgica*, 29 (1981), 1851-1863.
[22] OL Rocha, CA Siqueira, CA Siqueira, A Garcia, "Cellular/dendritic transition during unsteady-state unidirectional solidification of Sn/Pb alloys", *Materials Science and Engineering A*, 347 (2003) 59-69.
[23] T Siewert, S Liu, DR Smith, JC Madeni, "Database for Solder Properties with Emphasis on New Lead-free Solder", *Colorado: National Institute of Standards and Technology & Colorado School of Mines*, 77p (2002).